Research Square

Preprints are preliminary reports that have not undergone peer review.
They should not be considered conclusive, used to inform clinical practice,
or referenced by the media as validated information.

Linear Mixed Models for Longitudinal Analysis of In Vitro Root Growth in Solanum lycopersicum under Carbon Nanotube Treatments

Ernesto Solís-Delgado
Instituto Tecnológico de Tijuana
Monserrat Benítez-Radilla
Instituto Tecnológico de Tijuana
Y. Gochi-Ponce
Instituto Tecnológico de Tijuana
Rebeca Moreno-Santoyo
Instituto Tecnológico de Tijuana
Andrés García-Medina
andgarm.n@gmail.com

Instituto Tecnológico de Tijuana https://orcid.org/0000-0002-2198-880X

Research Article

Keywords: Holm method, Akaike Information Criterion (AIC), Bayesian information criterion (BIC), Seed-specific random effect

Posted Date: November 13th, 2026

DOI: https://doi.org/10.21203/rs.3.rs-11708658/v1

License: This work is licensed under a Creative Commons Attribution 4.0 International License.
Read Full License

Additional Declarations: The authors declare no competing interests.

Linear Mixed Models for Longitudinal Analysis of In Vitro Root Growth in *Solanum lycopersicum* under Carbon Nanotube Treatments

L. Ernesto Solís-Delgado[1], Monserrat Benítez-Radilla[1], Y. Gochi-Ponce[1], Rebeca Moreno-Santoyo[1], and Andrés García-Medina[1,*]

[1]Tecnológico Nacional de México/IT de Tijuana, Calz. del Tecnológico 12950, Tomás Aquino, Tijuana, 22414, Baja California, México.

[*]Corresponding author: andgarm.n@gmail.com

Abstract

This study evaluated root growth of tomato seedlings (*Solanum lycopersicum*) cultured in vitro on Murashige and Skoog (MS) medium under carbon nanotube treatments. We analyzed root growth using linear mixed-effects models (LMM) fitted by maximum likelihood to 1,350 observations from 90 seedlings across nine experimental groups over 15 days. Fixed effects described treatment-specific temporal trajectories, while a seedling-specific random intercept accounted for individual heterogeneity and within-seedling correlation. Among five candidate models, the treatment-specific quadratic model (M5) achieved the lowest AIC and BIC, supporting nonlinear growth trajectories with treatment-dependent slopes and curvature. Treatment differences were assessed through contrasts of predicted changes in root length between days 1 and 15,

using Wald tests with Holm adjustment to control the family-wise error rate across multiple comparisons. We found that T7 (functionalized multi-walled carbon nanotubes) and T8 (single-walled carbon nanotubes) showed the largest estimated growth improvement over the control, at 0.927 and 1.013 mm, respectively. Moreover, no statistically significant difference was detected between the two treatments after Holm adjustment, suggesting that the lower-cost option could be prioritized for further evaluation in scalable applications. These findings identify promising treatments for further evaluation and demonstrate the value of longitudinal modeling for assessing root growth.

Keywords:

Holm method; Akaike Information Criterion (AIC); Bayesian information criterion (BIC); Seed-specific random effect;

1 Introduction

The tomato is one of the most widely cultivated and consumed vegetables globally, owing to its high nutritional, economic, and agro-industrial value. It contains bioactive compounds such as lycopene, carotenoids, and vitamins A, C, and E, as well as essential minerals, making it a food of great interest for human health. Scientifically, the tomato has established itself as a biological model in plant research, as its genome is fully sequenced and its response to controlled *in vitro* conditions is well understood (The Tomato Genome Consortium 2012). Tomato cultivation (*Solanum lycopersicum*) ranks among the most valuable vegetable crops worldwide, with an estimated production of approximately 190 million tonnes covering more than five million hectares (Food and Agriculture Organization of the United Nations 2025; Klee and Resende 2020). Asia is the leading continent for tomato production, accounting for 62.6% of the total output, followed by the Americas (13.1%), Europe (12.2%), Africa (11.9%), and Oceania (0.2%). The tomato is a source of carotenoids, vitamins, glycoalkaloids, and other metabolites possessing antioxidant, anti-inflammatory, and antimutagenic properties (Chaudhary et al. 2018). Tomatoes are also a popular ingredient in various culi-

nary traditions; this has driven extensive breeding programs to develop an impressive array of tomato cultivars featuring a multitude of flavors, colors, and shapes (Domínguez et al. 2020).

In recent decades, the incorporation of nanotechnology into agriculture has opened up new opportunities to improve cultivation, germination, and productivity processes. Among the most widely studied nanomaterials, carbon nanotubes (CNTs) have garnered special attention due to their high mechanical strength, electrical conductivity, and chemical stability. Specifically, multi-walled carbon nanotubes (MWCNTs) consist of several concentric, rolled-up graphene layers that form a tubular structure On the other hand, single-walled carbon nanotubes (SWCNTs) are one-dimensional nanostructures composed of a single graphene sheet seamlessly rolled into a hollow cylindrical structure (Park et al. 2026). These characteristics make them potentially useful in biomedical, engineering, and biotechnological applications, including agriculture. The effect of MWCNTs depends on various factors, such as size, purity, synthesis method, exposure time, concentration, and number of walls. These variables can determine whether the nanotubes act as growth stimulators or as phytotoxic agents. It has been observed that high concentrations can be toxic, causing growth inhibition, morphological deformations, and alterations in cellular structure (Lin and Xing 2007; Lahiani et al. 2013; Aguilar-Vázquez et al. 2021; Gochi Ponce et al. 2026). Similarly, low doses of selenium and silicon nanoparticles stimulate growth and contribute to increased accumulation of phenolic compounds in crops such as chili pepper (*Capsicum annuum* L.) and oats (*Avena sativa* L.) (Sotoodehnia-Korani et al. 2020; Asgari et al. 2018). Furthermore, metal oxide-based nanomaterials—such as TiO2, Fe2O3, Al2O3, ZnO, and SiO2—have been shown to provide micronutrients and activate plant defense mechanisms, resulting in improved plant growth and development (Hussain et al. 2018). Similarly, foliar applications of cobalt oxide (Co3O4) and ZnO nanoparticles on crops such as rapeseed (*Brassica napus* L.) and common bean (*Phaseolus vulgaris* L.) have shown increases in growth, fresh weight, and yield, demonstrating the potential of these nanomaterials to promote plant development (Jahani et al.

2020; Salama et al. 2019). Further evidence comes from Ratnikova et al. (2015), who reported increased germination, root growth, and biomass in tomato following seed sonication combined with MWCNTs (50 mg L^{-1}). These effects may involve enhanced nanotube penetration and stress-related signaling that activates plant defense responses (Khodakovskaya et al. 2011; Zhao et al. 2020).

In tomato (*Solanum lycopersicum* L.), investigating the effects of MWCNTs is relevant to understanding their potential applications in plant biotechnology. Although previous studies have reported positive effects on seed germination and seedling growth, plant responses to carbon nanotubes may depend on their concentration, physicochemical properties, and experimental conditions. Therefore, further experimental evidence is required to characterize their effects and evaluate their potential applications in controlled in vitro culture systems Ratnikova et al. (2015); Villagarcia et al. (2012).

The objective of this study is to evaluate the effects of carbon nanotube treatments, including unmodified and nitrogen-modified MWCNTs at different concentrations, functionalized MWCNTs, and single-walled carbon nanotubes, on the in vitro root development of tomato seedlings cultured in Murashige and Skoog (MS) medium. The synthesis and detailed physicochemical characterization of the nanomaterials will be reported in a separate manuscript currently in preparation. Here, we focus on quantifying root development and assessing treatment-associated differences in growth over time.

Comparisons of root length at individual time points require an analysis that accommodates nonlinear trajectories and the dependence among repeated measurements from the same seedling. We therefore used linear mixed-effects models (LMMs) (Laird and Ware 1982; Verbeke 1997), comparing linear and quadratic mean structures with shared or treatment-specific slopes and curvature. The models included seedling-specific random intercepts to account for individual heterogeneity and the resulting within-seedling correlation. The central research question was whether the predicted mean change in root length between days 1 and 15 differed significantly among treatments, particularly relative to the control. The

main statistical contribution lies in the application of a longitudinal modeling framework to assess the effects of carbon nanotube treatments on tomato seedling root growth. This framework extends the evaluation beyond differences in root length at a single time point, providing a quantitative basis for identifying promising treatments for further investigation and potential applications in the agricultural industry.

The remainder of this paper is organized as follows. Section 2 describes the experimental data. Section 3 presents the linear mixed-effects modeling framework and statistical inference procedures. Section 4 reports the main results. Finally, Section 5 discusses the biological implications, statistical findings, and limitations of the study.

2 Experimental Data

Tomato seeds (*Solanum lycopersicum* L.) were cultured in vitro under controlled laboratory conditions and exposed to the experimental treatments summarized in Table 1.

Table 1: Culture medium composition and nanotube concentration by treatment.

Treatment	MS medium (%)	Nanotube type	Concentration (ppm)
Control	50	None	0
T1	40	None	0
T2	20	None	0
T3	20	MWCNT	50,000
T4	20	MWCNT	100,000
T5	20	MWCNT	200,000
T6	20	NTC-N	200,000
T7	20	NCMWF	200,000
T8	20	CNSW	200,000

Murashige and Skoog (MS) medium was used as the basal culture medium, with percentages expressed relative to the full-strength formulation. The experimental treatments included different types of carbon nanotubes. Multi-walled carbon nanotubes (MWCNTs) consist of multiple concentric cylindrical graphene layers. Nitrogen-doped carbon nanotubes (NTC-N) contain nitrogen atoms incorporated into their carbon structure. Functionalized

multi-walled carbon nanotubes (NCMWF) exhibit chemically modified surfaces, whereas CNSW corresponds to single-walled carbon nanotubes, consisting of a single cylindrical graphene layer. Half-strength MS medium (50% MS) without the addition of carbon nanotubes served as the control. These carbon nanomaterials were evaluated at different concentrations (parts per million, ppm) to assess their effects on root elongation in tomato seedlings under controlled *in vitro* conditions. The experimental design comprised one control and 8 treatments, with 10 seeds assigned to each treatment, and daily measurements from day 1 to day 15, yielding a total of 1,350 observations.

3 Statistical Analysis

Root growth was analyzed using LMMs to describe treatment-specific growth trajectories and take into account the repeated measurements within seedlings (Laird and Ware 1982; Verbeke 1997). Consider N observations from S seedlings assigned to J treatments. We have the LMM:

$$\mathbf{y} = \boldsymbol{\mu}^{(m)} + \mathbf{Z}\mathbf{u} + \boldsymbol{\varepsilon}, \qquad \boldsymbol{\mu}_m = \mathbf{X}^{(m)}\boldsymbol{\beta}^{(m)}, \tag{1}$$

where $\mathbf{y} \in \mathbb{R}^N$ contains the observed root lengths. The design matrix $\mathbf{Z} \in \mathbb{R}^{N\times S}$ contains indicator variables that map each observation to its seedling:

$$Z_{is} = \begin{cases} 1, & \text{if observation } i \text{ comes from seedling } s, \\ 0, & \text{otherwise.} \end{cases} \tag{2}$$

The random intercept u_s captures seedling-specific deviation from the mean trajectory for its treatment. The residual ε_i represents observation-level variation not explained by the model. We assume

$$\mathbf{u} \sim \mathcal{N}_S(\mathbf{0}, \tau^2\mathbf{I}_S), \qquad \boldsymbol{\varepsilon} \sim \mathcal{N}_N(\mathbf{0}, \sigma^2\mathbf{I}_N), \qquad \mathbf{u} \perp \boldsymbol{\varepsilon}, \tag{3}$$

where τ^2 describes between-seedling variability and σ^2 describes residual variability.

The mean vector $\boldsymbol{\mu}^{(m)} = \mathbf{X}^{(m)}\boldsymbol{\beta}^{(m)}$ contains the expected root length for each observation under a candidate model $m = \{M1, \ldots, M5\}$. Here $\mathbf{X}^{(m)}$ represents the fixed-effects design matrix encoding treatment and time, and $\boldsymbol{\beta}^{(m)}$ contains their coefficients. Let $\mu_{j,d}^{(m)}$ denote the mean root length under treatment j on day d. Time is centered as $x = d - d_c$, where d_c is the midpoint of the observation period, so that the intercept represents expected root length at that midpoint. The following candidate trajectories were considered in this work:

$$\mu_{j,d}^{(m)} = \begin{cases} a_j + bx, & m = \text{M1}, \\ a_j + b_j x, & m = \text{M2}, \\ a_j + bx + cx^2, & m = \text{M3}, \\ a_j + b_j x + cx^2, & m = \text{M4}, \\ a_j + b_j x + c_j x^2, & m = \text{M5}. \end{cases} \tag{4}$$

The models allow treatment-specific intercepts, where M1 and M2 assume common and treatment-specific linear slopes, respectively. M3 and M4 extend these structures with a common quadratic term, whereas M5 allows the quadratic coefficient to vary by treatment.

4 Results

The candidate models $m \in \{M1, M2, M3, M4, M5\}$ were fitted by maximum likelihood using the same observations and random-intercept covariance structure. The maximized log-likelihood and model-selection criteria are defined as Wood (2017)

$$\widehat{\ell}_m = \max_{\boldsymbol{\theta}_m} \log L_m(\boldsymbol{\theta}_m; \mathbf{y}), \tag{5}$$

$$\text{AIC}_m = -2\widehat{\ell}_m + 2k_m, \tag{6}$$

$$\text{BIC}_m = -2\widehat{\ell}_m + k_m \log n, \tag{7}$$

where $\boldsymbol{\beta}_m$ is the fixed-effect coefficient vector and $\boldsymbol{\theta}_m = (\boldsymbol{\beta}_m^{\mathsf{T}}, \tau_m^2, \sigma_m^2)^{\mathsf{T}}$ contains all estimated parameters. The marginal likelihood L_m is obtained by integrating out the random intercepts. Consequently, the total parameter count (including the random-intercept variance τ_m^2 and residual variance σ_m^2) is $k_m = p_m + 2$, where $p_m = \dim(\boldsymbol{\beta}_m)$. Akaike Information Criterion (AIC) and Bayesian information criterion (BIC) were calculated from the maximized marginal log-likelihood (see eqs.5-7).

Table 2 summarizes the comparison of the five temporal mean structures defined in Equation (4).

Table 2: Model selection in terms of maximum log-likelihood, AIC, and BIC.

m	p_m	l_m	AIC	BIC
M1	10	-100.586	225.172	287.667
M2	18	139.275	-238.551	-134.393
M3	11	79.134	-132.267	-64.565
M4	19	423.582	-805.165	-695.799
M5	27	512.670	-967.340	-816.312

The treatment-specific quadratic model (M5) achieved the lowest AIC and BIC and the highest maximized log-likelihood among the five candidate models. Its BIC was 120.512 units lower than that of the shared-curvature model (M4), the next-best candidate, and 681.918 units lower than that of the treatment-specific linear model (M2). These results supported selecting M5 for subsequent analyses, conditional on the assumed random-intercept covariance structure.

Figure 1 shows the fitted M5 trajectories with the 95% confidence interval bands for the estimated mean root length at each day. The linear M2 trajectories are superimposed for comparison purposes. The figure highlights the improvement in the quadratic model fits over the linear model. Actually, the quadratic model (M5) is able to capture the non-linear behavior of the first stages of root growth. The flexibility of the model to adapt to this kind of curvature is due to its quadratic term.

Treatment effects were summarized for M5 by the predicted change in population mean

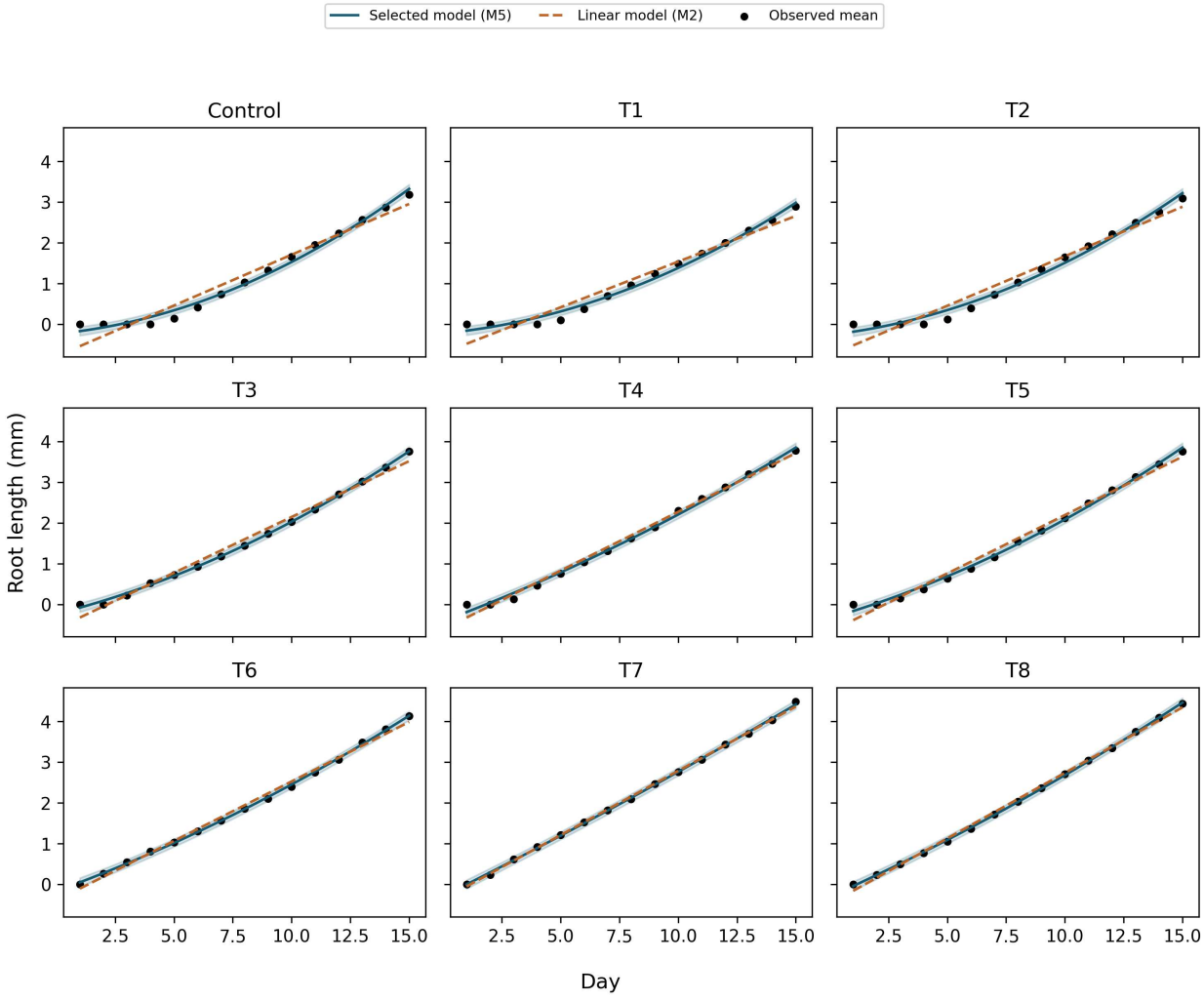


Figure 1: Estimated mean root-growth trajectories from the selected quadratic model M5 (blue solid curves), with 95% confidence interval bands. The red dashed lines represent the treatment-specific linear model M2, and points show observed treatment means.

root length between days 1 and 15, $\Delta_j = \mu_j(15) - \mu_j(1)$, where $\mu_j(d)$ denotes the population mean trajectory for treatment j. For each pair of treatments j and k, the null hypothesis $H_0 : \Delta_j - \Delta_k = 0$ was evaluated using an approximate two-sided Wald testWasserman (2004) Nevertheless, with one control and eight treatments, there were 36 pairwise comparisons. These multiple comparisons increase the risk of false positives, that is, detecting statistically significant differences between treatments when no true differences exist. To address this issue, Holm's procedureHolm (1979). was applied to adjust the p-values across comparisons, controlling the family-wise error rate at 5%. Table 3 presents the eight treatment–control contrasts. The $\widehat{D}_{ji} = \widehat{\Delta}_j - \widehat{\Delta}_i$, column reports the estimated difference in predicted growth change (in millimeters) between treatment j and treatment i. The 95% CI column gives the individual confidence interval. The final column reports the Holm-adjusted Wald-test p-values.

According to the results, T8 presents the largest estimated increase in root growth change relative to the control, followed by T7; both differences remained statistically significant after Holm adjustment. Although the estimated growth change was greater for T8 than for T7, their pairwise difference was not statistically significant (Table 3). Thus, the analysis did not detect a statistical difference between the NCMWF and CNSW treatments under the experimental conditions (see Table 1).

Figure 2 presents the estimated differences in predicted growth change between each treatment and the control $\widehat{D}_{j0}$, with individual 95% confidence intervals. The vertical dashed line at zero indicates no difference in predicted growth change relative to the control. Negative values indicate a smaller predicted growth change, whereas positive values indicate a larger change. The overlap for T7 and T8 highlights the fact that the pairwise difference was not statistically significant. Important to mention, that each interval estimates its own treatment-specific population contrast nor the family-wise correction.

Figure 3 summarizes the conditional residual diagnostics for M5. Conditional residuals were calculated as observed root lengths minus fitted values incorporating both fixed effects

Table 3: Estimated differences $\widehat{D}_{ji}$ in predicted growth change between days 1 and 15 estimated for fixed model structure M5. The reported p-values are Holm-adjusted across all 36 pairwise treatment comparisons.

A	B	$\widehat{D}_{ji}$ (mm)	Lower CI (95%)	Upper CI (95%)	p_{j0}^{Holm}
Control	T1	-0.352	-0.463	-0.241	***
Control	T2	-0.088	-0.199	0.023	0.601
Control	T3	0.348	0.237	0.459	***
Control	T4	0.548	0.437	0.659	***
Control	T5	0.523	0.411	0.634	***
Control	T6	0.599	0.488	0.711	***
Control	T7	0.926	0.814	1.037	***
Control	T8	1.013	0.901	1.124	***
T1	T2	0.264	0.153	0.375	***
T1	T3	0.700	0.589	0.811	***
T1	T4	0.900	0.789	1.011	***
T1	T5	0.874	0.763	0.986	***
T1	T6	0.951	0.840	1.063	***
T1	T7	1.277	1.166	1.389	***
T1	T8	1.365	1.253	1.476	***
T2	T3	0.436	0.325	0.547	***
T2	T4	0.636	0.525	0.747	***
T2	T5	0.610	0.499	0.722	***
T2	T6	0.687	0.576	0.799	***
T2	T7	1.013	0.902	1.125	***
T2	T8	1.101	0.989	1.212	***
T3	T4	0.200	0.089	0.311	**
T3	T5	0.174	0.063	0.286	*
T3	T6	0.251	0.140	0.363	***
T3	T7	0.577	0.466	0.689	***
T3	T8	0.665	0.553	0.776	***
T4	T5	-0.026	-0.137	0.086	0.726
T4	T6	0.051	-0.060	0.163	0.726
T4	T7	0.377	0.266	0.489	***
T4	T8	0.465	0.353	0.576	***
T5	T6	0.077	-0.034	0.188	0.601
T5	T7	0.403	0.292	0.514	***
T5	T8	0.490	0.379	0.601	***
T6	T7	0.326	0.215	0.437	***
T6	T8	0.413	0.302	0.524	***
T7	T8	0.087	-0.024	0.198	0.601

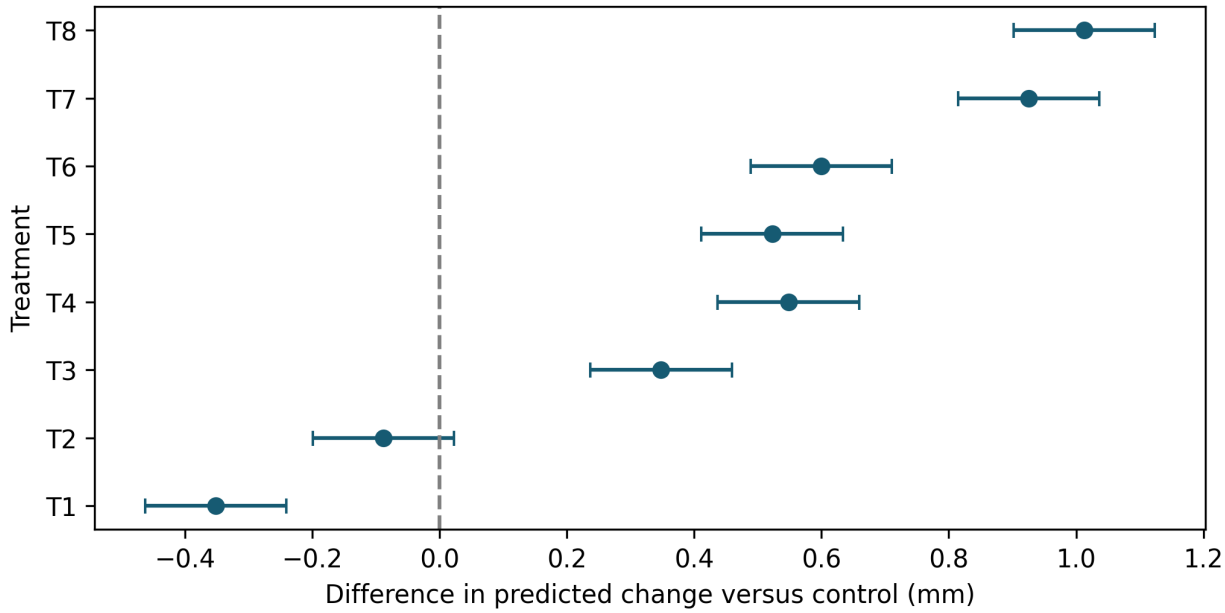


Figure 2: Differences in predicted growth change relative to the control.

and estimated seedling-specific random intercepts. The residual-versus-day plot shows residuals distributed around zero as assumed by the model, although their daily means exhibit a slight systematic temporal pattern. The normal Q–Q plot shows close agreement with the reference line in the central region, with small departures in both tails. Remaining temporal dependence was examined using pooled Pearson correlations between conditional residuals from the same seedling at lags of 1–7 days. Residual autocorrelation was strongly positive at lag 1 (approximately 0.79), declined with increasing lag, and became negative at longer lags, reaching approximately -0.45 at lag 7. These findings suggest that the random-intercept structure does not completely account for within-seedling temporal dependence. The diagnosis makes evident that further improvements are possible, yet at the cost of increasing the complexity and the number of parameters of the model.

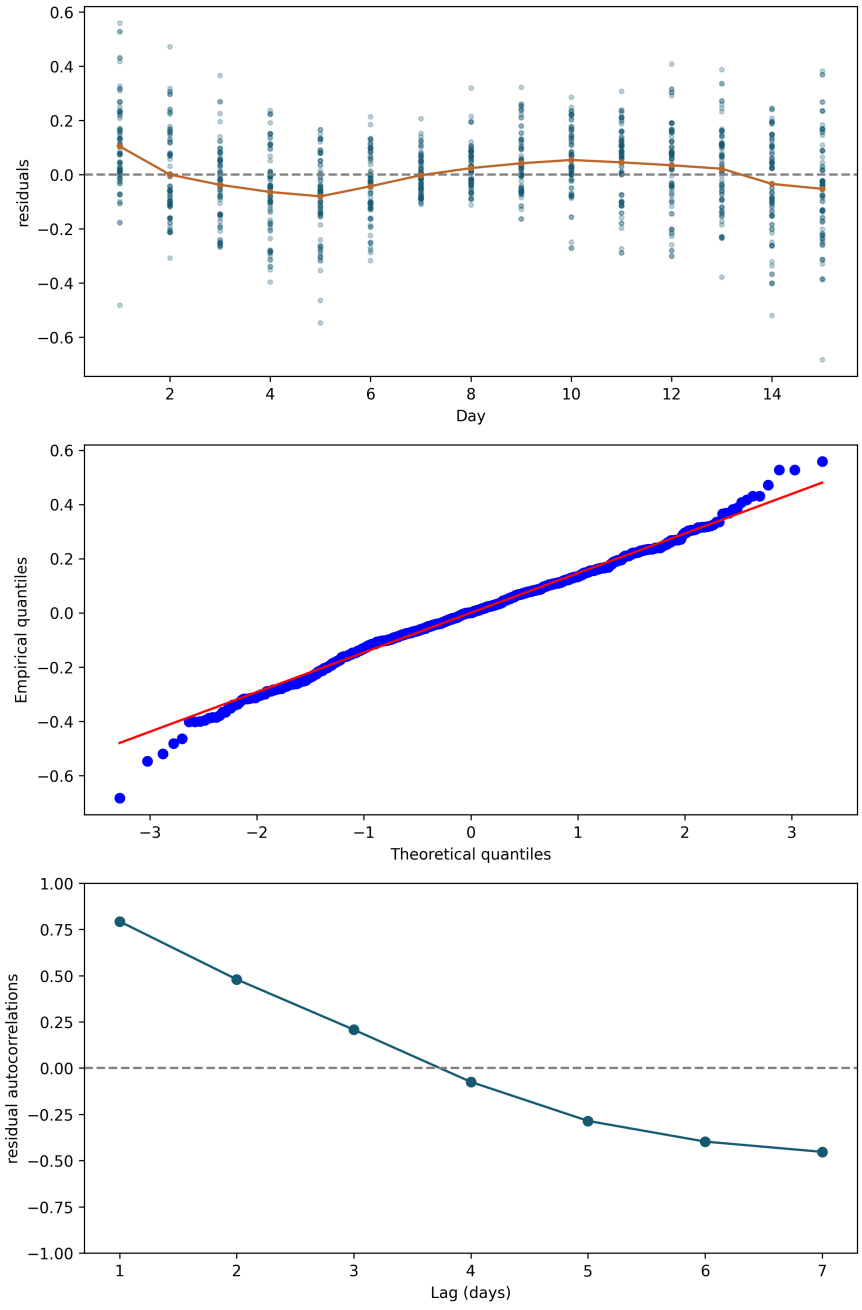


Figure 3: Residual diagnostics for M5. Top: residuals versus day (orange: daily mean). Middle: normal Q–Q plot. Bottom: pooled within-seedling lagged residual autocorrelations.

5 Conclusion

An LMM was used to account for fixed and random effects in tomato seedling root growth under different treatments. This approach provided estimates of the mean growth trajectories and predicted changes in root length over the observation period, together with their 95% confidence intervals. In particular, the LMM allowed us to assess the statistical significance of differences in predicted growth changes between treatments while accounting for repeated measurements within seedlings. This offered an analytical advantage over a classical one-way ANOVA applied to a single observation day, which can identify differences in mean root length between treatments but does not directly assess differences in growth trajectories.

An additional methodological contribution of the statistical analysis was the comparison of different fixed-effects structures for the mean growth trajectory, including linear and quadratic models with common slopes or curvature, as well as models with treatment-specific coefficients. Among the candidate models, M5, which allowed both linear and quadratic coefficients to vary by treatment, achieved the highest maximized log-likelihood and the lowest BIC and AIC. It was therefore selected as the preferred model within the candidate set, balancing goodness of fit and model complexity. Visual inspection of the fitted trajectories provided complementary support for this choice, showing that M5 captured the nonlinear growth pattern observed during the early stages of the observation period.

After M5 was selected as the preferred model, the predicted mean change in root length between days 1 and 15 was estimated for each treatment. Pairwise Wald tests with Holm-adjusted p-values were used to assess differences between treatments, controlling the family-wise error rate across the 36 comparisons. T7 and T8 showed the largest estimated increases in root growth relative to the control, with differences in predicted change of 0.927 and 1.013 mm, respectively. However, their confidence intervals overlapped, and the direct pairwise comparison was not statistically significant after Holm adjustment.

These findings identify T7 and T8, consisting of the addition of functionalized multi-walled carbon nanotubes (NCMWF) and single-walled carbon nanotubes (CNSW), respec-

tively, as promising candidates for further evaluation of technical and commercial feasibility. Both treatments showed significantly greater predicted increases in root length than the control over the observation period. No statistically significant difference was detected between them after Holm adjustment, suggesting that the lower-cost option could be prioritized for further assessment in a scalable engineering application.

Further research should extend the experimental period to determine whether the observed advantage in root growth persists through plant maturity and translates into improved plant development and yield. Evaluations of safety, environmental effects, and economic feasibility would also be needed before considering commercial implementation.

Data Availability

All data generated or analysed during this study are included in this published article

Conflict of Interest Statement

The authors have no competing interests to declare that are relevant to the content of this article.

Declaration of AI-assisted work.

ChatGPT (OpenAI) was used to assist with language editing, mathematical exposition, code review, and bibliography formatting. All AI-assisted material was reviewed and verified by the authors, who assume full responsibility for the accuracy and integrity of the manuscript.

References

Aguilar-Vázquez J, del Socorro Pina-Canseco M, Gochi-Ponce Y, Pérez-Santiago AD (2021) Efecto anti-proliferativo en líneas celulares de cáncer de mama y cervico-uterino causado por nanotubos de carbono múltipared-lectina de phaseolus lunatus var. silvester baudet. Revista Biomédica 32:87–97. https://doi.org/10.32776/revbiomed.v32i2.863.

Asgari F, Majd A, Jonoubi P, Najafi F (2018) Effects of silicon nanoparticles on molecular, chemical, structural and ultrastructural characteristics of oat (avena sativa l.). Plant physiology and biochemistry 127:152–160. https://doi.org/10.1016/j.plaphy.2018.03.021.

Chaudhary P, Sharma A, Singh B, Nagpal AK (2018) Bioactivities of phytochemicals present in tomato. Journal of Food Science and Technology 55:2833–2849. https://doi.org/10.1007/s13197-018-3221-z.

Domínguez M, Dugas E, Benchouaia M, Leduque B, Jiménez-Gómez JM, Colot V, Quadrana L (2020) The impact of transposable elements on tomato diversity. Nature communications 11:4058. https://doi.org/10.1038/s41467-020-17874-2.

Food and Agriculture Organization of the United Nations (2025) FAOSTAT: Crops and livestock products. https://www.fao.org/faostat/en/#data/QCL. Data for 2024. Accessed 14 October 2026.

Gochi Ponce Y, Guerrero Llamas ME, Solís Delgado LE, Villarreal Gómez LJ, Méndez Valenzuela E (2026) Evaluación in vitro de nanomateriales de carbono para aplicaciones biotecnológicas. Pädi Boletín Científico de Ciencias Básicas e Ingenierías del ICBI 14:318–323. https://doi.org/10.29057/icbi.v14iEspecial.15389.

Holm S (1979) A simple sequentially rejective multiple test procedure. Scandinavian journal of statistics 65–70. https://doi.org/10.2307/4615733.

Hussain A, Ali S, Rizwan M, ur Rehman MZ, Javed MR, Imran M, Chatha SAS, Nazir R (2018) Zinc oxide nanoparticles alter the wheat physiological response and reduce the cadmium uptake by plants. Environmental Pollution 242:1518–1526. https://doi.org/10.1016/j.envpol.2018.08.036.

Jahani M, Khavari-Nejad RA, Mahmoodzadeh H, Saadatmand S (2020) Effects of cobalt oxide nanoparticles (co3o4 nps) on ion leakage, total phenol, antioxidant enzymes activities and cobalt accumulation in brassica napus l. Notulae Botanicae Horti Agrobotanici Cluj-Napoca 48:1260–1275. https://doi.org/10.15835/nbha48311766.

Khodakovskaya MV, de Silva K, Nedosekin DA, Dervishi E, Biris AS, Shashkov EV, Galanzha EI, Zharov VP (2011) Complex genetic, photothermal, and photoacoustic analysis of nanoparticle-plant interactions. Proceedings of the National Academy of Sciences 108:1028–1033. https://doi.org/10.1073/pnas.1008856108.

Klee HJ, Resende MF (2020) Plant domestication: reconstructing the route to modern tomatoes. Current Biology 30:R359–R361. https://doi.org/10.1016/j.cub.2020.02.072.

Lahiani MH, Dervishi E, Chen J, Nima Z, Gaume A, Biris AS, Khodakovskaya MV (2013) Impact of carbon nanotube exposure to seeds of valuable crops. ACS applied materials & interfaces 5:7965–7973. https://doi.org/10.1021/am402052x.

Laird NM, Ware JH (1982) Random-effects models for longitudinal data. Biometrics 963–974. https://doi.org/10.2307/2529876.

Lin D, Xing B (2007) Phytotoxicity of nanoparticles: inhibition of seed germination and root growth. Environmental pollution 150:243–250. https://doi.org/10.1016/j.envpol.2007.01.016.

Park J, Kim C, Kim MJ (2026) Selective synthesis of single-walled carbon nanotubes in cvd

via wall number control: a review. Materials Today Nano 35:100952. https://doi.org/10.1016/j.mtnano.2026.100952.

Ratnikova TA, Podila R, Rao AM, Taylor AG (2015) Tomato seed coat permeability to selected carbon nanomaterials and enhancement of germination and seedling growth. The Scientific World Journal 2015:419215. https://doi.org/10.1155/2015/419215.

Salama DM, Osman SA, Abd El-Aziz M, Abd Elwahed MS, Shaaban E (2019) Effect of zinc oxide nanoparticles on the growth, genomic dna, production and the quality of common dry bean (phaseolus vulgaris). Biocatalysis and Agricultural Biotechnology 18:101083. https://doi.org/10.1016/j.bcab.2019.101083.

Sotoodehnia-Korani S, Iranbakhsh A, Ebadi M, Majd A, Ardebili ZO (2020) Selenium nanoparticles induced variations in growth, morphology, anatomy, biochemistry, gene expression, and epigenetic dna methylation in capsicum annuum; an in vitro study. Environmental Pollution 265:114727. https://doi.org/10.1016/j.envpol.2020.114727.

The Tomato Genome Consortium (2012) The tomato genome sequence provides insights into fleshy fruit evolution. Nature 485:635–641. https://doi.org/10.1038/nature11119.

Verbeke G (1997) Linear mixed models for longitudinal data. In Verbeke G, Molenberghs G (eds), *Linear Mixed Models in Practice: A SAS-Oriented Approach*, volume 126 of *Lecture Notes in Statistics*, pages 63–153. Springer. https://doi.org/10.1007/978-1-4612-2294-1_3.

Villagarcia H, Dervishi E, de Silva K, Biris AS, Khodakovskaya MV (2012) Surface chemistry of carbon nanotubes impacts the growth and expression of water channel protein in tomato plants. Small (Weinheim an der Bergstrasse, Germany) 8:2328–2334. https://doi.org/10.1002/smll.201102661.

Wasserman L (2004) All of Statistics: A Concise Course in Statistical Inference. Springer Texts in Statistics. Springer. https://doi.org/10.1007/978-0-387-21736-9.

Wood SN (2017) Generalized additive models: an introduction with R. chapman and hall/CRC. https://doi.org/10.1201/9781315370279.

Zhao L, Lu L, Wang A, Zhang H, Huang M, Wu H, Xing B, Wang Z, Ji R (2020) Nanobiotechnology in agriculture: use of nanomaterials to promote plant growth and stress tolerance. Journal of agricultural and food chemistry 68:1935–1947. https://doi.org/10.1021/acs.jafc.9b06615.